Legacy-Agnostic Band Integration Approach: A Cost-Effective and Seamless C+l-Band Optical Network Migration

MohammadHasan Shammakhi , Farhad Arpanaei , *Member, IEEE*, Hamzeh Beyranvand , and Hamid Sheikhzadeh

Abstract—This paper addresses the escalating demand for enhanced data transmission rates and increased network capacity in elastic optical networks. We propose a novel legacy-agnostic band integration approach for cost-effective and seamless C+Lband optical network migration, focusing on a "pay-as-you-grow" (PaYG) strategy to optimize capital expenditure (CAPEX). This approach leverages advanced modeling techniques, including the enhanced generalized Gaussian noise (EGGN) model, to account for inter-channel stimulated Raman scattering (ISRS) and other nonlinear effects, ensuring optimal quality of transmission (QoT). Through extensive simulations on real-world network topologies, we compare the performance of various PaYG algorithms against a traditional Day-One (DO) approach, demonstrating significant gains in throughput and CAPEX efficiency. Notably, the proposed PaYG-WAR (PaYG-With All Reconfigurations) outperforms other strategies, maximizing throughput while minimizing the deployment of costly infrastructure components. Our results provide valuable insights for telecom operators seeking a financially viable and practical solution for migrating optical networks to C+Lband operation. Specifically, PaYG-WAR achieves 20% higher throughput compared to DO and PaYG-WoR (PaYG-Without Reconfigurations) and 17% more than PaYG-WFR (PaYG-With Full Reconfigurations), while requiring 25% less CAPEX than DO-CHB (DO-Channel Based). These findings underscore the potential of PaYG-WAR in facilitating efficient, cost-effective network upgrades to meet next-generation communication demands.

Index Terms—Capital expenditure (CAPEX), C+L-band network, enhanced generalized Gaussian noise (EGGN) model, pay-as-you-grow (PaYG), quality of transmission (QoT).

I. INTRODUCTION

ONVENTIONAL single-band wavelength division multiplexing (WDM) optical networks, predominantly

Received 25 November 2024; revised 23 March 2025, 17 June 2025, and 13 July 2025; accepted 13 August 2025. Date of publication 19 August 2025; date of current version 2 October 2025. The work of Farhad Arpanaei was supported in part by EU-funded 6G SNS SEASON Project under Grant 101096120, in part by EU-funded FLEX-SCALE Project under Grant 101096909, in part by Spanish-funded Fund-date-Redes Project under Grant PID2022-1366840B-C21, and in part by TUCAN6-CM Project under Grant TEC-2024/COM-460 funded by the Community of Madrid (ORDER 5696/2024). (Corresponding Author: Hamzeh Beyranvand.)

MohammadHasan Shammakhi, Hamzeh Beyranvand, and Hamid Sheikhzadeh are with the Department of Electrical Engineering, Amirkabir University of Technology (Tehran Polytechnic), Tehran 159163-4311, Iran (e-mail: mh.shammakhi@aut.ac.ir; beyranvand@aut.ac.ir; hsheikh@aut.ac.ir).

Farhad Arpanaei is with the Department of Telematic Engineering, Universidad Carlos III de Madrid (UC3M), Leganés, 28911 Madrid 159163-4311, Spain (e-mail: farhad.arpanaei@uc3m.es).

Color versions of one or more figures in this article are available at https://doi.org/10.1109/JLT.2025.3600265.

Digital Object Identifier 10.1109/JLT.2025.3600265

utilizing the C-band with a limited bandwidth of approximately 4.8 THz, are rapidly approaching their capacity limits due to the escalating demand for enhanced data transmission rates and increased network capacity [1]. This surge in demand is driven by the proliferation of emerging technologies such as 6G, cloud computing, and the Internet of Things (IoT) [2]. Multi-band optical networks (MBON), which extend beyond the traditional C-band to encompass the extended C+L-band (12 THz), the C+L+S-band (20 THz), and potentially further into the U+L+C+S+E+O-band (59 THz), offer an effective strategy for capacity scaling by leveraging the low loss regions of the optical spectrum [3]. This approach enables significant capacity expansion without necessitating extensive alterations to the existing network infrastructure. The primary motivation for adopting MBON is not only to accommodate higher data throughput but also to ensure long-term scalability, meeting the evolving demands of next-generation communication systems. This allows for the seamless deployment of high-capacity services and supports the continuous growth of global data traffic [4].

However, while emerging technologies offer numerous benefits, they also present significant challenges, particularly in terms of implementation, compatibility with legacy systems, and maintaining interoperability. This is especially critical for backbone optical networks, where the sensitivity of national and global traffic relies heavily on these infrastructures [5]. Therefore, upgrading these networks from legacy technologies to nextgeneration solutions is a primary concern for telecom operators (Telcos). Their goal is to achieve seamless, hitless migration or upgrading between technologies, ensuring minimal disruption. Although recent efforts have successfully commercialized the C+L-band [6], and ongoing work is expanding into the L+C+Sband and beyond it [7], the key question remains: how can this migration be implemented effectively? While some research such as [4], [8], [9], [10], [11], [12], [13], [14], [15], [16] addressed when and where Telcos should upgrade their topologies to migrate from C-band networks to MBONs, the real challenge lies in how this upgrade can be accomplished seamlessly. The motivation of this paper is to address this crucial question.

We propose a novel legacy-agnostic band integration approach for cost-effective and seamless MBON migration, focusing on a "pay-as-you-grow" (PaYG) strategy to optimize capital expenditure (CAPEX) that ensures the quality of service of

0733-8724 © 2025 IEEE. All rights reserved, including rights for text and data mining, and training of artificial intelligence and similar technologies. Personal use is permitted, but republication/redistribution requires IEEE permission. See https://www.ieee.org/publications/rights/index.html for more information.

existing services, i.e., bitrate remains unaffected during the implementation of new bands. This approach not only guarantees service continuity but also optimizes cost efficiency throughout the upgrade process. Furthermore, the Enhanced Generalized Gaussian Noise (EGGN) model is used for Inter-channel Stimulated Raman Scattering (ISRS)-aware network planning. The EGGN model accurately accounts for ISRS effects, enhancing the accuracy of capacity planning and power optimization (band-agnostic power optimization) in MBON. This approach surpasses previous studies that either neglected ISRS or relied on less precise models for migration.

Comparative analysis of the proposed migration scenarios reveals a nuanced trade-off between immediate capacity expansion and long-term cost efficiency. While the Day-One (DO) approach offers immediate access to maximum bandwidth, it incurs substantial upfront costs. Conversely, the PaYG strategies, particularly PaYG-With all reconfiguration (WAR), demonstrate superior long-term cost-effectiveness by incrementally upgrading the network based on actual demand, resulting in optimized resource allocation and reduced CAPEX. Although PaYG-WAR may involve more frequent reconfigurations, its superior throughput and lower overall infrastructure costs ultimately outweigh this operational overhead, making it a compelling alternative to DO deployments for efficient MBON migration.

The most significant contributions of this paper are: (i) Novel Legacy-Aware Band Integration (LABI) for PaYG Networks: The paper introduces a novel approach to seamlessly integrate legacy C-band services with new L-band capacity during a PaYG upgrade. This contrasts with prior work that often neglected the complexities of integrating existing services, resulting in potentially disruptive upgrades. The LABI method incorporates multi-layer service reconfiguration and Generalized Signal-to-Noise-Ratio (GSNR)-agnostic channel assignment for efficient service migration. (ii) Comprehensive Comparison of PaYG Strategies with varying Reconfiguration Levels: The paper systematically compares five distinct PaYG upgrade algorithms (differentiated by reconfiguration strategies: no reconfiguration, partial, full, and all), offering a nuanced analysis of their respective trade-offs regarding throughput, CAPEX, and operational complexity. This goes beyond previous works which typically focused on only one or two approaches. (iii) Optimized multi-layer grooming for efficient resource utilization: The proposed algorithms incorporate multi-layer grooming techniques to optimize spectrum usage and minimize the number of required line card interfaces during network upgrades, improving overall cost-effectiveness compared to previous studies. The integration of multi-layer grooming with ISRS-aware network planning and LABI represents a significant advancement. The PaYG-WAR algorithm emerges as particularly efficient. (iv)Comprehensive techno-economic analysis: The paper conducts a thorough comparison of different migration strategies across multiple real-world network topologies, considering various factors including throughput, CAPEX, and operational complexity, to provide a holistic evaluation of their feasibility and efficacy. It should be noted that while this paper focuses on the C+L-band, the proposed upgrading approaches can be extended to cover frequency bands beyond the C+L-band.

TABLE I ABBREVIATIONS USED IN THIS PAPER

ASE	Amplified Spontaneous Emission
CAPEX	Capital Expenditure
CHB	Channel Based
CU	Cost Unit
DO	Day-One
DO-CHB	DO-Channel Based
DO-MinG	DO-Minimum GSNR
EDFA	Erbium-Doped Fiber Amplifier
EGGN	Enhanced Generalized Gaussian Noise
FLP	Flat Launch Power
FRP	Flat Receive Power
GSNR	Generalized Signal-to-Noise Ratio
ILA	Inline Amplifier
IoT	Internet of Things
IP/MPLS	Internet Protocol/Multiprotocol Label Switching
ISRS	Inter-Channel Stimulated Raman Scattering
LABI	Legacy-Aware Band Integration
LCI	Line Card Interface
LP	Lightpath
MBON	Multi-Band Optical Networks
MCS	Multi-Cast Switches
MFL	Modulation Format Level
MinG	minimum channel's GSNR
NLI	Nonlinear Interference
PaYG	Pay-as-You-Grow
PaYG-MinG	PaYG-Minimum GSNR
PaYG-WAR	PaYG-With All Reconfiguration
PaYG-WFR	PaYG-With Full Reconfigurations
PaYG-WoR	PaYG-Without Reconfigurations
PaYG-WPR	PaYG-With Partially Reconfiguration
QAM	Quadrature Amplitude Modulation
QoS	Quality of Service
QoT	Quality of Transmission
RoB	ROADM-on-blade
SDN	Software-Defined Networking
URT	Unserved Residual Traffic
WAR	With All-Reconfigurations
WDM	Wavelength Division Multiplexing

In Table I, all abbreviations used in this paper are listed to help the reader refer to key terms more easily.

This paper provides a comprehensive exploration of C+L-band optical network migration. After a concise introduction that establishes the context and motivation, Section II reviews the state-of-the-art network upgrading strategies, contrasting the DO and PaYG approaches. Section III outlines the system model and underlying assumptions, including the EGGN model. In Section IV, the core contribution is presented, introducing and elaborating on five proposed PaYG algorithms with varying degrees of reconfiguration. Section V discusses the simulation setup and presents results, offering a detailed performance analysis of the algorithms across key metrics such as blocking rate, throughput, CAPEX, and component counts, using three distinct network topologies. Finally, Section VI concludes the paper, summarizing the key findings and discussing their implications for network planning and upgrade strategies.

II. STATE-OF-THE-ART IN UPGRADING STRATEGIES FOR SINGLE-BAND OPTICAL NETWORKS

Two key strategies have been proposed for upgrading C-band WDM optical networks to MBONs: the DO and the PaYG [4],

[8], [17], [18]. In the DO method, suitable for greenfield deployments, it is assumed that an MBON, such as C+L-band optical network is established from the outset of the network's lifecycle. This ensures immediate access to the full capacity of several bands, providing ample bandwidth for future demand. Nevertheless, it is acknowledged that this approach is financially expensive, considering the costs associated with deploying a multi-band transmission system such as the in-line amplifiers (ILA) across all links from the outset [10], [11], [17]. On the other hand, the PaYG approach to network upgrading in terms of infrastructure and capacity is aligned with actual demand and usage [4], [8], [18]. Instead of a multi-band transmission system from the beginning of the network, including excess capacity that might not be immediately utilized, PaYG allows Telcos to incrementally scale to MBON based on evolving requirements. In this model, businesses pay for the network resources and capacity they need at the moment, so at the beginning of networks, there is no need for an extra band transmission system [13]. This approach provides CAPEX efficiency by avoiding overprovisioning and allows adaptation to market dynamics [4], [8]. A PaYG algorithm for upgrading C-band WDM networks to C+L-band and/or 3-core multi-core fiber links was proposed in [19]. This algorithm, however, assumed that the link undergoing the upgrade was out of service, necessitating rerouting of existing traffic. Crucially, the approach in [19] lacked the LABI techniques introduced in this paper. These LABI techniques, by checking all affected established services during the upgrade process, are vital for maintaining both quality of service (QoS, e.g., bitrate) and quality of transmission (QoT, e.g., GSNR) for rerouted traffic. Furthermore, [19] did not account for the impact of ISRS on amplified stimulated emission (ASE) noise calculation and power optimization, a factor addressed in our work.

The approach presented in [15] explores service reconfiguration using a batch process, upgrading multiple links to C+L-band at once and reallocating C-band services to the L-band to free up resources. While this method offers a straightforward solution, it results in increased CAPEX due to the simultaneous upgrade of multiple links, and limits all services to operate within a single band. In contrast, our proposed PaYG methodology enables more flexible, granular upgrades, allowing for the selective upgrade of individual links. This flexibility ensures that new service requests can be provisioned through hybrid paths, where some links in a lightpath are upgraded to C+L-band while others remain in C-band, optimizing resource allocation and reducing costs. Furthermore, [15] does not address the effects of ISRS in ASE noise or incorporate the challenges associated with partially loaded C+L-band configurations or pre-tilt power optimization. These gaps could lead to instability in network performance, as fluctuations in GSNR may arise due to power profile adjustments on individual links. Our method overcomes these issues by incorporating practical assumptions for MBONs, where idle channels are filled with shaped ASE noise, thus better simulating real-world conditions [29]. Moreover, we leverage an advanced power optimization approach as outlined in [23], [24], which allows for more efficient resource utilization.

While batch-based upgrading methods, similar to those discussed in [15], were also explored in previous studies [13], [14], these approaches primarily focus on fully loaded, distance-adaptive scenarios. Alternatively, [21] presents a combination of heuristic and integer linear programming strategies for upgrading, offering a techno-economic analysis of CAPEX differences. However, unlike our work, which optimizes power for each link's concurrent state, the PaYG approach in [8] focuses on end-of-life systems, requiring a larger initial CAPEX and not accounting for reconfigurations during system operation.

Our work significantly advances existing strategies by addressing the limitations of batch upgrading, incorporating more realistic power optimization techniques, and offering a cost-effective solution that avoids the high initial investments typically associated with traditional methods. Key differences between the state-of-the-art upgrading strategies and our approach are summarized in Table II.

III. SYSTEM MODEL AND INITIAL ASSUMPTIONS

According to cutting-edge modem technologies for optical Flexponders, the transceivers in this work utilize flexible modulation format levels, soft decision forward error correction, and variable bit rates [25]. Therefore, based on the GSNR of each channel, the transmission rate of the corresponding transceivers can be adaptively tuned by adjusting the modulation format or the spectral efficiency of the transceivers. This flexibility can be provided by uniform standard M-quadrature amplitude modulation (QAM) with adaptive variable code rate, probabilistic constellation shaping, or time-domain hybrid-format technologies [26].

Moreover, flexibility in the transmission rate of the transceivers enables traffic grooming in the optical layer instead of the Internet Protocol/Multiprotocol Label Switching (IP/MPLS) layer. Traffic grooming in the optical layer is managed by the orchestrator, which controls the IP/MPLS and optical layer software-defined networking (SDN) controller agents. Therefore, when a new request arrives or re-configuration is required the spare capacity of the already established TRxs between the same source and destination is utilized. If the spare capacity is lower than the required bitrate, a new TRx must be deployed. Furthermore, we assume that the nodes are equipped with super C-band (6 THz) at the beginning of the network and super L-band (6 THz) transceivers when the L-band channels are required.

The ILA sites are equipped with C-band erbium-doped fiber amplifiers (EDFA) for the super C-band and super L-band channels. The ASE-shaped noise is considered for the idle channels based on the commercialized scenario to guarantee the power-gain profile consistency [27], [28]. Furthermore, ILA sites utilize dynamic gain equalizers for optimal launch power per span, leveraging the hyper-accelerated power optimization strategy from [23], [24]. We assume the use of cutting-edge modular ROADM-on-blade (RoB) technology. Each RoB incorporates embedded optical time-domain reflectometry, optical channel monitoring, and dynamic gain equalizers to provide

Main Features of Upgrading Algorithms in Literature	[19]	[9]–[11]	[8]	[13], [14]	[20], [21]	[22]	[15]	This paper
Pay as You Grow	√	×	√	×	√	×	√	√
Demand Optimization	×	√	√	√	×	√	×	√
Band-Agnostic Power Optimization	×	×	√	×	×	×	×	√
Multi-Layer Service Reconfiguration	×	×	×	×	×	×	×	√
ISRS-Aware ASE Noise Modeling	×	×	√	×	×	×	×	√
Multi-Layer Grooming	×	×	×	×	×	×	×	√
GSNR-Agnostic Channel Assignment	√	√	×	×	×	×	×	√
Legacy-Agnostic Band Integration	×	×	×	√	×	×	×	√

TABLE II SUMMARY OF THE RELATED WORKS

telemetry data for SDN control and power optimization [29]. These assumptions ensure the support of band-agnostic power optimization, LABI, and GSNR-agnostic channel assignment algorithms, all crucial for next-generation MBONs.

In this study, we adopt a comprehensive physical-layer model that accounts for key impairments impacting transmission quality in elastic optical networks. The model is designed to realistically capture both deterministic and statistical effects on signal degradation, ensuring accurate QoT estimation. Specifically, we consider the following major components: (i) ASE noise introduced by EDFAs, (ii) nonlinear interference (NLI) effects including self-phase modulation (SPM), cross-phase modulation (XPM), four-wave mixing (FWM), and ISRS, (iii) transceiver SNR limitations, (iv) filtering penalties introduced by cascaded wavelength selective switches (WSSs), and (v) a margin to account for equipment aging.

For NLI estimation, although the GGN model is widely adopted, its enhanced version, EGGN, introduces a novel aspect in C- to C+L-band migration, a scenario not previously explored for network migration. Conventional noise models assume homogeneous conditions, but in multi-band networks, factors such as ISRS, chromatic dispersion variations, ASE noise, and amplifier power profiles become increasingly significant. The EGGN model addresses these challenges by incorporating signal power variations and modulation format dependencies, enabling more accurate performance evaluation [30], [31]. Additionally, its frequency-dependent parameters, such as chromatic dispersion and loss coefficients, Raman gain, and ASE noise, make it well-suited for MBONs. The validation of the EGGN model was also conducted through field trials [32]. Thus, we use the EGGN model to ensure precise QoT estimation while enabling optimized parameter tuning and resource allocation for C- to C+L-band upgrades.

To compute the GSNR for a lightpath (LP) on channel i ($GSNR_{LP}^i$), we adopt the incoherent NLI accumulation model, which is commonly used for uncompensated optical transmission links [33]. Accordingly, the $GSNR_{LP}^i$ in dB is given by (1):

$$GSNR_{LP}^{i}|_{dB} = 10\log_{10} \left[\left(SNR_{ASE}^{-1} + SNR_{NLI}^{-1} + SNR_{TRx}^{-1} \right)^{-1} \right] - \sigma_{Flt}|_{dB} - \sigma_{Ag}|_{dB}, \quad (1)$$

where $SNR_{\text{ASE}} = \Sigma_{s \in S} P_{\text{tx}}^{s+1,i}/P_{\text{ASE}}^{s,i}$ and $SNR_{\text{NLI}} = \Sigma_{s \in S} P_{\text{tx}}^{s+1,i}/P_{\text{NLI}}^{s,i}$. Moreover, $P_{\text{tx}}^{s+1,i}$ is the launch power at the beginning of span s+1, $P_{\text{ASE}}^{s,i} = n_{\text{F}} h f^i (G^{s,i}-1) R_{\text{ch}}$ is noise power caused by the EDFA equipped with the dynamic gain equalizer,

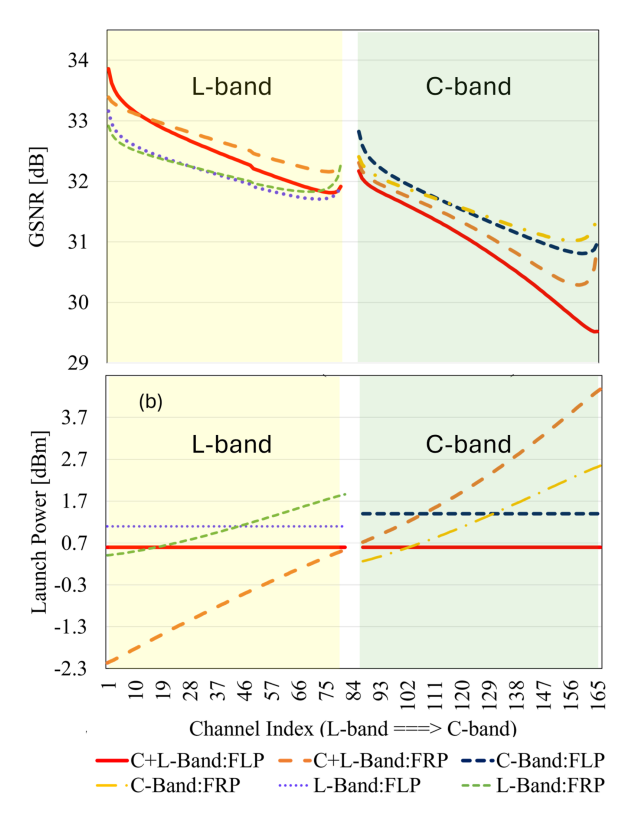


Fig. 1. Effect of FRP and FLP algorithm on GSNR Profiles in MBONs: (a) GSNR (b) Launch power profiles.

and NLI noise power $(P_{\rm NLI}^{s,i})$ is calculated from (2) in [30] based on EGGN model. Moreover, $n_{\rm F},\ h,\ f^i,\ G^{s,i}=P_{\rm tx}^{s+1,i}/P_{\rm rx}^{s,i},\ S,$ and $R_{\rm ch}$ are the EDFA's noise figure, Plank's coefficient, channel frequency, frequency center of the spectrum, EDFA's gain, set of spans, and channel symbol rate, respectively. $P_{\rm rx}^{s,i}$ is the received power at the end of span $s.\ SNR_{\rm TRx},\ \sigma_{\rm Flt},\ \sigma_{\rm Ag}$ are the transceiver SNR, SNR penalty due to WSS filtering, and SNR margin due to the aging.

It is worth mentioning the WSS filtering penalty captures the signal quality degradation caused by the cumulative effect of filtering in cascaded WSS used in ROADMs. This phenomenon leads to progressive spectral narrowing and signal distortion. The value of this penalty is selected based on insights from recent studies analyzing WSS-induced performance degradation in real-world optical networks [23], [34], [35].

Fig. 1 illustrates the GSNR profile and related power profiles for different MBON scenarios over a 70 km transmission. Six scenarios are C-band, L-band, and C+L-band with flat launch

power (FLP) optimization and flat receive power (FRP) optimization method based on the hyper-accelerated power optimization strategy [23], [24]. In the hyper-accelerated power optimization strategy, the maximum capacity of each span is calculated under a fully-loaded assumption, which is practical for MBONs [6], [28]. The optimal power and GSNR profiles for all spans in the C-band and C+L-band are then determined. Consequently, when calculating the end-to-end GSNR and corresponding modulation format based on (1), we use the optimal span GSNR and power profiles in either the C-band or C+L-band, depending on whether the active link operates in the C-band or C+L-band. As shown in Fig. 1, the FRP algorithm increases the average GSNR profile by approximately 0.9 dB, resulting in a more uniform GSNR profile. This also flattens the received power, which in turn ensures a consistent optical signalto-noise ratio profile. In this case, the launch power includes a tilt controlled by the dynamic gain equalizers. Additionally, results indicate that the GSNR of the C-band and L-band scenarios is lower than the GSNR of these bands in the C+L-band scenario, demonstrating that a fully-loaded assumption with ASE-noise shaped channels is essential for MBONs.

In our study, the L-band is gradually activated, starting with only the C-band active. This approach leads to a QoS (bitrate) degradation for C-band channels as new L-band channels are added. In other words, during network upgrades from the C-band to the C+L-band, some links may contain only C-band channels while others have both C and L bands. Using (1), we calculate the GSNR of each channel in each span based on whether it is in the C-band only or includes both C and L bands.

When a link is upgraded from the C-band to the C+L-band, the GSNR of each channel decreases due to ISRS. This GSNR reduction during C-to-C+L migration makes it crucial to assess whether the updated GSNR falls below the threshold for the current modulation level. If it does, channel reconfiguration is needed to avoid BER degradation in the connection. In such cases, if the required capacity is defined as $C_{\rm Req}$ and the maximum capacity based on the current GSNR related to modulation format level (MFL) m is represented as C_m , the unserved residual traffic (URT) due to a reduced modulation format level can be calculated by (2):

$$C_{\text{URT}} = C_{\text{Reg}} - C_m, \tag{2}$$

If C_{URT} is greater than zero, channel reconfiguration becomes necessary. The choice of reconfiguration method directly affects the channels' feasibility for future demands. Therefore, suitable upgrade algorithms are essential to maintain network performance and ensure service reliability for established connections in MBONs.

IV. PROPOSED STRATEGIES FOR UPGRADING TO C+L-BAND

In this section, we examine two widely used strategies for scaling a network to meet growing demand. We start by outlining the DO approach, followed by a detailed exploration of five incremental, or PaYG, strategies. This includes a range of methods for updating GSNR values and configuring channels, from worst-case and channel-based GSNR assessments to strategies

with varying degrees of reconfiguration: no reconfiguration, partial reconfiguration, full reconfiguration, and comprehensive channel reconfiguration.

A. DO Approaches

In the DO approach, we start with the assumption that all links are upgraded to the C+L-band from the network's inception. This means that when establishing connections to serve demands, we have the flexibility to assign each demand to either the C-band or L-band based on the available network capacity. Additionally, we can establish connections between any two nodes using different paths, providing multiple options for serving demand in the network. This approach applies to greenfield network planning when the initial traffic from day one is substantial, requiring Telcos to implement C+L-band systems from the start. Therefore, the GSNR of all LPs are calculated in advance by assuming that the C+L-band equipment in the optical terminals and optical line systems is deployed. For MFL selection, we consider two approaches: the minimum channel's GSNR of each band (MinG) and the channel-based approach (CHB), in which the MFL of each channel is selected based on its related GSNR.

B. Pay-As-You-Grow (PaYG)

The PaYG approach in optical networks offers greater flexibility and cost efficiency compared to DO planning, which relies on long-term traffic forecasts and often results in overprovisioning, high upfront CapEx, and underutilized resources. In contrast, PaYG supports incremental network expansion driven by actual demand, thereby improving resource utilization, reducing financial risk, and aligning infrastructure upgrades with ongoing technological advancements. This adaptability facilitates the seamless integration of innovations such as higher-order modulation formats for C-band transmission and multi-band operation to maximize spectrum utilization. While a comprehensive analysis of energy consumption and overall Operational Expenditure is beyond the scope of this study, it is worth noting that, as reported in [36], the energy consumption per terabit remains nearly constant when upgrading from C-band to C+L-band. This indicates that the proposed multiband migration strategy can substantially enhance capacity with minimal energy overhead. Nonetheless, a key challenge of the PaYG paradigm lies in managing legacy lightpaths. Whereas DO planning incorporates design margins to future-proof the network, PaYG emphasizes spectral efficiency, often operating with tighter margins to better accommodate evolving traffic demands [17].

This paper introduces an optimal PaYG algorithm that preserves QoT during incremental upgrades while enabling network operators to scale up to C+L-band optical networks as demand evolves. By incorporating a more accurate physical-layer model and realistic network assumptions, our approach ensures efficient resource allocation and a comprehensive evaluation against existing DO and PaYG strategies. However, the upgrade structure, specifically the process of migrating links from C-band to C+L-band within the network, is crucial. This subsection outlines five C+L-band PaYG upgrade methods, discussing our expectations along with their benefits and drawbacks. Fig. 2

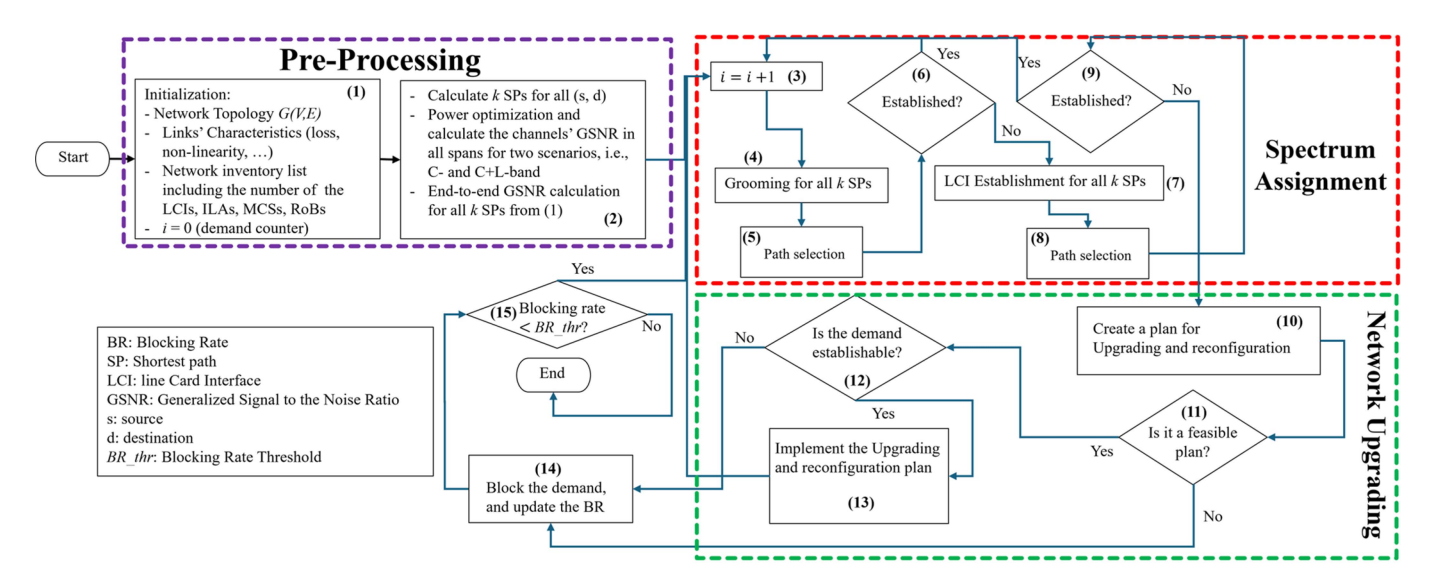


Fig. 2. The flowchart of the proposed PaYG methods.

presents a general flowchart of the PaYG steps. The proposed PaYG approach includes the following components: (i) Band-Agnostic Power Optimization, (ii) Multi-Layer Service Reconfiguration, (iii) ISRS-Aware ASE Noise Modeling, (iv) EGGN - Enhanced Generalized Gaussian Noise, (v) - Multi-Layer Grooming, (vi) GSNR-Agnostic Channel Assignment, and (vii) LABI - Legacy-Agnostic Band Integration.

As the first step, the algorithm requires legacy network topology, fiber characteristics, and infrastructure specifications such as RoBs, Multi-Cast Switches (MCSs), ILAs, and Line Card Interface (LCIs). The algorithm operates by first determining k=3 shortest candidate paths for each given source-destination (s, d) pair. Additionally, we pre-calculate the optimum power and the related GSNR of all channels of the spans in each candidate path for both C- and C+L-band scenarios based on the FRP optimization algorithm proposed in [23]. Next, it utilizes the pre-calculated GSNR of individual spans (refer to (1) for details) to calculate the end-to-end GSNR of each channel within these identified paths for the C-band and C+L-band scenarios. Finally, based on the calculated end-to-end GSNR and a defined threshold, the algorithm determines the MFL and the related bitrate for each channel. Similar to the DO approaches, we employ two methods for assigning modulation based on GSNR, as explained above: MinG and CHB.

A key consideration is that, instead of imposing a fixed maximum transmission distance, our approach dynamically evaluates the channel-based GSNR to determine the transmission reach and select the appropriate modulation format for each path. This method provides a more accurate assessment of network performance by considering both the maximum reach distance and real-time channel conditions, rather than relying on a fixed distance estimated based on worst-case GSNR assumptions [23].

Following the pre-processing steps, the spectrum assignment steps (3-8), prioritize C-band channels to check the possibility of grooming and establishing new LCIs based on the first fit

spectrum assignment. This assignment continues until no C-band channel within the three candidate paths can accommodate a new demand's required bitrate by grooming or establishing new LCIs.

In the network upgrading steps (10-12), the algorithm prioritizes links for upgrade based on the following criteria: i) the link must currently operate in the C-band, ii) upgrading the link must enable it to accommodate the new demand and iii) links with fewer idle channels and shorter lengths are prioritized over those with greater capacity and longer spans. If multiple links meet these conditions, shorter links are given precedence.

Once a suitable link is identified, it is added to the *migration plan*. The *migration plan* represents a stage where the selected link(s) undergo upgrades and reconfigurations within a digital twin network, ensuring feasibility before deployment in the real-world network.

Following link selection, the end-to-end GSNRs for all active lightpaths along the updated path (including the upgraded link) are recalculated. Additionally, GSNRs for unassigned channels across the three candidate paths are re-evaluated for different connections. Based on these updated values, new channel capacities are determined. Finally, any existing assignments exceeding the updated capacity threshold (as per (2)) must be reconfigured. This reconfiguration involves either shifting them to available free channels or utilizing channels with sufficient grooming capacity to maintain network efficiency.

After reconfiguring the network, the algorithm verifies whether the updated state meets both capacity and GSNR threshold requirements. If no channel exceeds its capacity (i.e., the URT remains non-positive for all channels), the reconfiguration is deemed valid, and the algorithm proceeds to establish the target demand (step 12). A successful establishment triggers the application of the migration plan, finalizing the upgrade and serving the demand in step 13.

However, if the reconfiguration is infeasible or the demand cannot be established, the changes within the migration plan

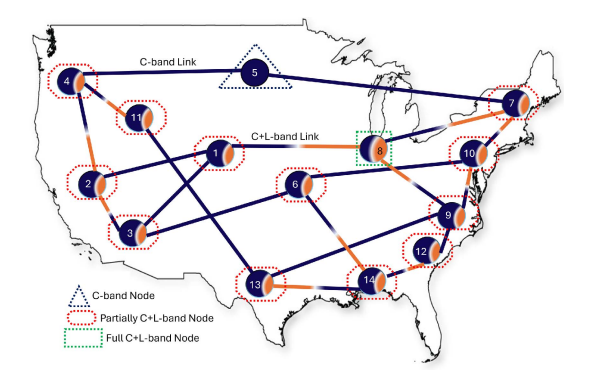


Fig. 3. Partially upgrading links to be C+L-band,.

must be reverted. The algorithm then attempts to upgrade an alternative link within the path and reconfigure channels with positive URT. If no further upgrade candidates are available in the path, the list of upgraded links is discarded, and the process shifts to evaluating the next potential path for serving the demand.

This iterative process continues until the demand is successfully accommodated. If no feasible upgrade configuration is found in step 12, the algorithm ultimately blocks the demand. Notably, the algorithm continues serving new demands until the blockage ratio (B_R) falls below the predefined threshold (B_{thr}) . As the final step, once this threshold is reached, the serving procedure terminates.

It is important to note that all lightpaths in the end-to-end connection retain their original configurations, including frequency band and channel allocation, ensuring that no lightpath requires frequency or band switching along its route. This guarantees seamless signal transmission without the need for band-switching mechanisms or wavelength conversion, as C-and L-band lightpaths remain confined to their respective bands and are routed exclusively through corresponding components (e.g., amplifiers and switches).

Consider the network topology shown in Fig. 3 as an example. This network consists of 14 nodes and 20 links, with navy blue lines representing C-band links and navy blue-orange lines representing C+L-band links. Suppose that a new demand arises from node 3 to node 10. The three shortest paths connecting these nodes are: $(3 \rightarrow 6 \rightarrow 10)$, $(3 \rightarrow 1 \rightarrow 8 \rightarrow 9 \rightarrow 10)$, and $(3 \rightarrow 1 \rightarrow 8 \rightarrow 7 \rightarrow 10)$. Additionally, we assume none of these paths currently have an idle feasible channel or a channel with sufficient grooming capacity to accommodate the demand. To address this, the network must be upgraded. Focusing on the shortest path $(3 \rightarrow 6 \rightarrow 10)$, we identify two candidate links for upgrade: L(3,6) and L(6,10). Assume L(6,10) has fewer free channels (i.e., is likely busier) and shorter, thus, it becomes the first choice for C-band to C+L-band migration. This link is then added to the migration plan and upgraded. However, establishing the L-band can reduce the GSNR of the already established C-band channels, impacting the bitrate capacity potential of the C-band channels of all connections that their candidate paths traverse this upgraded link. The algorithm implements the migration plan by upgrading L(6, 10). This upgrade may

necessitate reconfiguring some channels based on their GSNR. If the current configuration is invalid (indicating that the demand still cannot be served), the algorithm adds L(3,10) to the upgrade list and proceeds to upgrade both L(6,10) and L(3,10). If upgrading the first path $(3 \to 6 \to 10)$ does not lead to a valid network configuration after reconfiguration, the algorithm moves on to the second path $(3 \to 1 \to 8 \to 9 \to 10)$. Here, the only upgrade option is link L(3,1). Similar to the first path, the algorithm checks for a valid reconfiguration after upgrading L(3,1). If successful (meaning the demand can be served), the upgrade is complete. However, if a valid reconfiguration is not achievable for the second path, the same will likely apply to the third path $(3 \to 1 \to 8 \to 7 \to 10)$ as it also requires upgrading L(3,1). In this case, with no valid migration plan found, the new demand is blocked, and the network waits for the next request.

It is important to note that the proposed PaYG algorithm, like the DO, determines channel capacity by computing GSNR in two ways: MinG and CHB. Additionally, different reconfiguration methods, each with its advantages and disadvantages, will be explained. These methods include partial reconfiguration, full reconfiguration, and all-reconfiguration approaches. Detailed explanations of these methods will follow.

- 1) PaGY-MinG: In this approach, we start by assuming that the network initially consists only of C-band links. We calculate the minimum GSNR values in the C-band to serve as reference points for all channels, while taking into account potential GSNR degradation due to future L-band deployment from the outset. Based on these GSNR values, MFLs are assigned to C-band channels within each connection's path. The PaYG algorithm establishes demands until there are no more channels that meet the requirements of the new demand. Upon encountering new demand that cannot be accommodated by existing channels, the network undergoes a targeted upgrade to a C+L-band transmission system in specific nodes and links. Since the highest margin has been accounted for from the outset, adding L-band links does not require reconfiguration of already established lightpaths.
- 2) PaYG-Without Reconfiguration (PaYG-WoR): This algorithm, similar to other PaYG methods, starts with a C-bandonly network. However, it differs by incorporating C+L-band assumptions when calculating span GSNR. This approach aims to avoid reconfiguration during network upgrades. The lightpath GSNR is derived based on the anticipated C+L-band capability. Unlike the PaYG-MinG approach, where the GSNR is computed based solely on the minimum GSNR, this method considers a margin for when the L-band is activated, ensuring that already established lightpaths are not affected but based on CHB method. While this method enables serving new demands until the blocking threshold is reached without requiring immediate reconfiguration, it has the downside of underestimating the C-band's capacity at the beginning of the network's life. This underestimation, caused by the C+L-band assumptions for GSNR estimation, leads to earlier network upgrades.

In the following, we will introduce three PaYG algorithms based on the CHB-MFL selection strategy that require reconfiguration to reduce the initial GSNR margin, increase the network's spectrum efficiency, and postpone the need for network upgrades. Before that, let us explain an illustrative example that

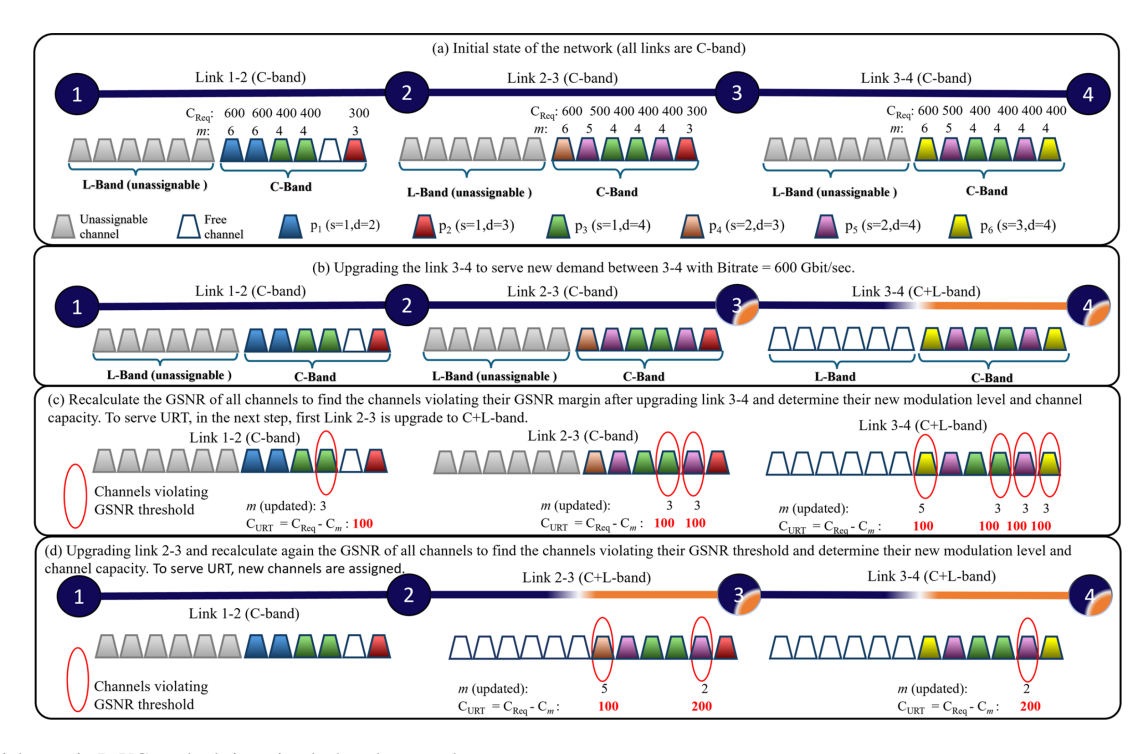


Fig. 4. Initial steps in PaYG methods in a simple 4-node example.

clarifies the idea behind our proposed algorithm. Fig. 4 is a simple example illustrating the details of the PaYG algorithm and its different reconfiguration strategies. In this example, we consider a network with four nodes interconnected by three links, L(1, 2), L(2,3), and L(3,4)—all currently utilizing C-band components. The first row (Fig. 4(a)) shows established demands within each channel. The color coding of each channel corresponds to the connection between the given source-destination (s, d) pairs. Suppose we upgrade L(3,4) to C+L-band (Fig. 4(b)). This upgrade changes the GSNR of each C-band channel, impacting the GSNR of established lightpaths passing through this link (see Fig. 4). Consequently, the maximum channel capacity (C_{Req}) can fluctuate due to the GSNR degradation, which results in a decrease in the MFL. Channels with new MFL lower than the initial assigned MFL are outlined in red, i.e., lightpaths p_3 , p_5 , and p_6 , indicating the need for reconfiguration (Fig. 4(c)). The URT capacities are calculated and saved to the migration plan. Therefore, as shown in Fig. 4(d), in the next step, the link L(2,3) needs to be upgraded to C+L-band to serve the URT of affected lightpaths $(p_3, p_5, \text{ and } p_6)$ from the previous step. After this upgrade, the new affected connections must be determined by recalculating GSNR. As shown in Fig. 4(d), the MFLs of p_4 and p_5 are degraded, and its URT must be served with a reconfiguration strategy. It should be noted that although the GSNR of lightpath p_2 has degraded, it still has enough GSNR margin, and its MFL remains unchanged.

Now we are ready to explain three strategies for the reconfiguration stage to establish the URT and the new demand based on the illustrative example in Fig. 5.

3) PaYG With Full Reconfiguration (PaYG-WFR): PaYG-WFR prioritizes a complete transition of any channel requiring

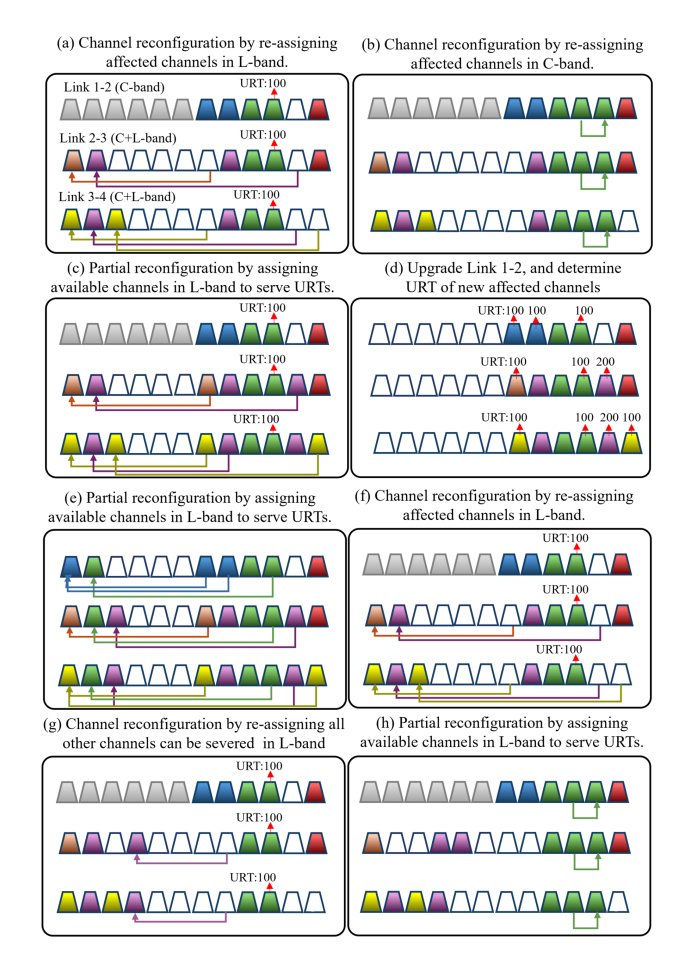


Fig. 5. Reconfiguration steps in (a)–(b) PaYG-WFR, (c)–(e) PaYG-WPR, and (f)–(h) PaYG-WAR methods.

reconfiguration after the upgrade from the C- to the L-band. This approach not only directly addresses the immediate reconfiguration needs but also significantly enhances the network's future flexibility.

The steps of the reconfiguration method in PaYG-WFR are depicted in Fig. 5(a)–(b). The first step involves reconfiguring the affected lightpaths in the C-band that can be moved to the L-band, as shown in Fig. 5(a). This process targets the brown channel (p_4) and one of the purple channels (p_5) , as both are affected and have URT. Initially, the purple channel is moved to an idle channel, followed by the reconfiguration of the brown channel. In the second step, lightpaths requiring reconfiguration that still have some C-band links in their path must be addressed. These lightpaths must be reconfigured to another C-band channel, as shown in Fig. 5(b). Depending on capacity, this may involve moving the entire channel or a portion. In this example, there is no available C-band channel to reconfigure the entire channel, so we reallocate the URT to another C-band channel. As shown, 100 Gbps of the green channel (p_3) is moved to an idle channel to bring it within the feasible bitrate range. It is worth mentioning that complete channel migration to the L-band during reconfiguration offers several advantages. First, for a partially C+L-band path, this approach frees up more C-band channels. This not only optimizes current network resource utilization but also creates more flexibility for efficiently accommodating future demands.

4) PaYG-With Partially Reconfiguration (PaYG-WPR): This algorithm closely resembles PaYG-WFR, except for its reconfiguration procedure. In the reconfiguration stage, the algorithm allocates only the URT to the L-band channels, while the initial host channel retains the remaining bitrate.

Fig. 5(c)–(e) illustrates the PaYG-WPR reconfiguration steps for the network example in Fig. 4. Let's consider upgrading link L(2-3) and link L(3-4) to C+L-band (shown in Fig. 4(d)). While most channels can be reconfigured to accommodate the new GSNR and serve their URT, the URT of the affected channel p_3 (green channel) cannot be served as shown in Fig. 5(e). To address this issue, we upgrade link L(1-2) to C+L-band as well (Fig. 5(d)). However, this additional upgrade might introduce new capacity violations in other channels. The final solution involves assigning new channels specifically for the URT portions of each violated channel (marked in Fig. 5(e)). With this reconfiguration, all channels are now within capacity, and the process is considered successful. However, despite network support for grooming, this reconfiguration model imposes limitations on future demands. Some channels are initially designated for specific source-destination pairs and may not be fully utilized, increasing the probability of inefficiency in channel usage. Additionally, there might be a need to reconfigure some partially C+L-band channels to other C-band channels. In such cases, only URT is reconfigured. Consequently, some other C-band channels are labeled for grooming and may not accept additional connections.

5) PaYG With All Reconfigurations (PaYG-WAR): In this strategy, our goal is to leverage the maximum capacity available in the L-band. The initial steps align with PaYG-WPR and

PaYG-WFR except for the reconfiguration phase. When upgrading certain links from the C-band to the C+L-band, all feasible channels from the C-band are reconfigured to the L-band. This approach significantly increases available C-band channels for future demands, delaying the need for the next network upgrade. It is important to highlight that if, during a C+L-band upgrade, a channel requires reconfiguration but channel capacity is insufficient, we only reconfigure URT to maintain QoT.

To further clarify this approach, consider Fig. 4(d) as the initial state. We aim to upgrade two links in the L-band, resulting in some violated channels based on the new GSNR. In the first step, we reconfigure the channels that have the reconfiguration condition to the L-band (Fig. 5(f)). Then, we proceed to reconfigure all possible C-band channels to the L-band, as shown in Fig. 5(g). Next, we search for free channels in the C-band for the violated channels that cannot be reconfigured to the L-band. Consequently, they need to be reconfigured to other available Cband channels, as shown in Fig. 5(h). The PaYG-WAR algorithm offers several potential advantages. It can support higher bitrates, which translates to greater network capacity. Additionally, it can delay the need for network upgrades, consequently reducing the number of C+L-band RoBs and ILAs. However, this approach may come at the cost of more frequent reconfigurations and the need for additional LCIs in the L-band after upgrades are performed.

The proposed PaYG algorithms follow a greedy approach, making locally optimal decisions at each step to efficiently address C+L-band optical network migration. This strategy enables rapid network reconfiguration while balancing computational efficiency and performance. Compared to more complex methods, PaYG demonstrates superior resource utilization, enhanced network stability, and lower migration costs, making it a highly effective solution for real-world optical networks.

Table III illustrates the main characteristics of different reconfiguration strategies in optical networks. It highlights how each approach manages spectrum allocation, reconfiguration scope, and spectral efficiency. The table provides a comparative view of their impact on network adaptability, resource utilization, and the balance between C-band and L-band usage.

V. SIMULATION SETTING AND RESULTS

A. Physical Layer Parameters

To compute the GSNR of the network, practical parameters about the network's physical layer are utilized. Coherent flexible transceivers are employed, operating at a fixed baud rate of 64 GBaud, variable modulation format levels, and possessing soft-decision Forward Error Correction capability. These transceivers are used with a ratio of 2 for transmitting different modulation formats, accommodating both high and low bit-rate transmission schemes to suit varying network demands.

The LCIs feature a transceiver noise coefficient of 36 dB and a spectral bandwidth equivalent to six frequency slots (i.e., 6×12.5 GHz, totaling 75 GHz). A guard band of 500 GHz is maintained between the C and L bands. Furthermore, the analysis includes a 2-dB aging SNR margin, fixed EDFAs

TABLE III
THE MAIN CHARACTERISTICS OF THE CONSIDERED ALGORITHMS

Algorithm	Main Characteristics
DO-MinG	 It is assumed that all the links are initially C+L. The GSNR is obtained based on the lowest GSNR value in each frequency band.
DO-CHB	 It is assumed that all the links are initially C+L. The GSNR is obtained based on the channel GSNR value.
PaYG-MinG	 The GSNR is obtained based on the lowest GSNR value in each frequency band. If full reconfiguration is not possible, partial reconfiguration is applied.
PaYG-WoR	 The GSNR is obtained based on a fully loaded C+L-band network. It does not require any reconfiguration.
PaYG-WPR	 Only the URT part of each affected lightpath is reconfigured (partially). It uses less L-band capacity after reconfiguration. L-band is the primary target for reconfiguration.
PaYG-WFR	 The entire lightpath is reconfigured if the URT value is positive. Only the affected lightpath is reconfigured. Reconfiguration is performed as needed to maintain QoT. It frees up more C-band channels for future demands. L-band is the primary target for reconfiguration. If full reconfiguration is not possible, partial reconfiguration is applied.
PaYG-WAR	 Reconfigure to L-band as much as possible. Both affected and non-affected lightpaths are reconfigured. Priority is given to the affected lightpaths for reconfiguration. It significantly frees up C-band channels for future demands. L-band is the primary target for reconfiguration. If full reconfiguration is not possible, partial reconfiguration is applied.

with noise figure values of 4.5 and 5.5 dB in the C- and L-bands, respectively, and a before Forward Error Correction BER threshold of 1.5×10^{-2} . Based on these specified parameters, the GSNR thresholds corresponding to modulation format orders m=1-6 (equivalent to bitrates of 100, 200, 300, 400, 500, and 600 Gbit/s, respectively) are computed as 3.45, 6.5, 8.4, 12.4, 16.5, and 19.34 dB, respectively [4]. In

scenarios where the requested bitrate exceeds the maximum capacity of a single channel for a given modulation format, the request is accommodated over several channels, all utilizing the same modulation format. Additionally, the study includes three backbone networks: the Spanish backbone (SPNB14) with 14 nodes and 22 links, the Japanese backbone (JPNB12) with 12 nodes and 17 links, and the United States backbone (USB14) with 14 nodes and 22 links. The motivation for selecting these networks is to represent small, medium, and ultra-long-distance networks, respectively, with SPNB, JPNB, and USB backbones. These networks offer average link lengths of 301 km, 437 km, and 927 km, and connection distances of (656, 893, 1100) km, (929,1159,1394) km, and (1966,2713,3308) km, respectively, for paths k=1,2,3.

B. Results and Discussion

This section delves into the impacts of each upgrading strategy from C-band to C+L-band across various dimensions. We thoroughly compare each algorithm's throughput under different bitrate blocking rates. Additionally, we analyze the number of RoBs, MCSs, ILAs, LCIs, and reconfigurations during network upgrading. Furthermore, we examine the number of upgraded links to C+L-band in the network. These analyses are performed on a computing system equipped with a 13th Gen Intel Core i5-13450HX, 2400 MHz, 10 Cores, 16 Logical Processors, and 16GB of memory.

1) Blocking Rate Versus Throughput: A key performance metric in optical networks is throughput, defined as the number of successfully established demands under specific blocking rate thresholds. Fig. 6 illustrates the blocking rate as a function of increasing system throughput. In this evaluation, the network is simulated using randomly generated demand sequences, applying each algorithm under identical conditions. To ensure statistical validity, multiple demand realizations are used, mimicking a Monte Carlo-style randomized testing environment.

The first four methods represent widely adopted approaches in conventional network designs. Among them, CHB-based algorithms tend to offer higher throughput, particularly under fixed configurations. However, when upgrade and reconfiguration flexibility is introduced, the PaYG-WAR method consistently outperforms all other strategies across all evaluated topologies. While PaYG-WFR also demonstrates strong throughput performance, it provides complementary benefits—such as reduced fragmentation and lower reconfiguration complexity—that make it a valuable option depending on the operational goals. These benefits are further explored in later sections through other performance metrics.

Focusing on Fig. 6(a), which presents the results for the USB14 network, three performance tiers emerge. The highest-performing method is PaYG-WAR, which consistently achieves superior throughput. The middle tier includes DO-CHB, PaYG-WoR, and PaYG-WFR, while the remaining methods form the lower tier. PaYG-based methods initially operate in the C-band and defer C+L-band upgrades, often routing demands via the second or third shortest paths. Although these paths are typically longer and span more links—resulting in higher risk of

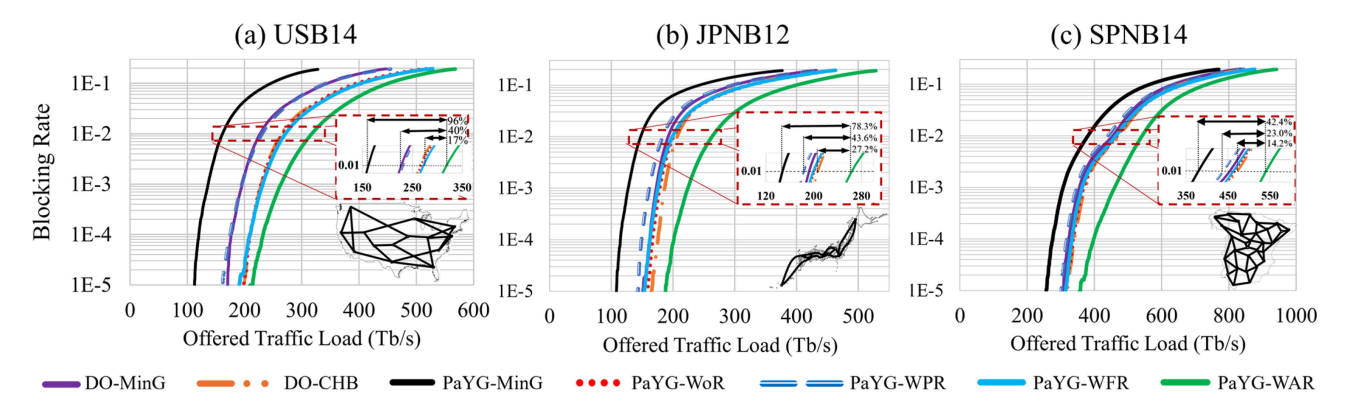


Fig. 6. Established traffic of different approaches at various blocking rates in USB14, JPNB12, and SPNB14 networks.

blocking—the initial C-band capacity is limited, prompting this behavior. Notably, at a 1% blocking rate, PaYG-WAR establishes 17% more demands than DO-CHB and PaYG-WoR, and 40% more than DO-MinG in the USB14 network. This highlights the algorithm's strong capability to maximize throughput under stringent constraints.

In the JPNB12 network (Fig. 6(b)), where links are shorter and the number of spans is lower, higher GSNR values enable the use of advanced modulation formats with minimal degradation. As a result, the performance gap between mid-tier and top-tier methods is narrower. Nevertheless, PaYG-WAR still maintains its lead.

In SPNB14 (Fig. 6(c)), where path lengths are short and the topology supports a more balanced load distribution, the performance among the middle and top-tier algorithms is even closer. Here, DO-CHB and PaYG-WoR deliver relatively strong results, though PaYG-WAR again achieves the highest throughput.

Several network parameters affect the performance of DO-MinG and PaYG-MinG algorithms. Based on the GGN model, longer spans and links increase GSNR variance, which reduces the effectiveness of MinG-based methods due to their reliance on minimum GSNR as a reference. While equal power allocation and identical topologies make link length a dominant factor for MinG methods, other factors like power distribution can have a greater impact on PaYG algorithms. Moreover, PaYG performance depends on how closely alternative paths resemble the shortest one. In symmetric topologies with similar path lengths, PaYG performs better due to its strategy of deferring C+L upgrades and utilizing more diverse C-band paths.

PaYG-WPR is especially sensitive to GSNR degradation and reconfiguration overhead, since it prioritizes preserving existing assignments over relocating lightpaths, unlike PaYG-WFR and PaYG-WAR. In dense networks or after significant GSNR losses during C+L upgrades, WPR struggles due to limited residual capacity, while WFR and WAR benefit from freeing C-band space through L-band migration. Topology plays a key role: in compact networks like JPN12, alternative paths are similar, minimizing algorithm differences. In larger, more heterogeneous networks like USB14, GSNR penalties, amplifier noise, and nonlinearities accumulate over long links and spans, magnifying differences between algorithms and stressing the importance of capacity aware design.

TABLE IV PERFORMANCE IMPACT OF NETWORK TOPOLOGY PARAMETERS ACROSS DIFFERENT ALGORITHMS

Algorithm	Increase Link Length	Shortest Paths Similarity	Power Diversity		
DO-MinG	_	0			
DO-CHB	0	0	0		
PaYG-MinG	_	+			
PaYG-WoR	0	++	0		
PaYG-WPR	_	+	0		
PaYG-WFR	_	+	0		
PaYG-WAR	_	+	0		

The effects of these parameters on performance are summarized in Table IV. The symbol '+' indicates improved performance, '-' indicates degraded performance, and '0' denotes no significant impact.

The USB14 and SPNB14 networks are larger and have longer links and spans compared to JPNB12. While detailed information on reconfiguration events is provided in the following sections, it is worth noting that the number of reconfigurations in PaYG-WPR for USB14 is lower than in SPNB14. As a result, PaYG-WPR achieves a more acceptable blocking rate in SPNB14 when compared to other algorithms, particularly in contrast to its performance in USB14.

Moreover, in SPNB14, the second and third shortest paths are more comparable in length to the shortest path. This leads to a more balanced distribution of traffic and contributes to performance results that are closer to those achieved by the DO-based algorithms. However, since the power levels are optimized individually for each network, the power variation cannot be directly compared based on topology, as it is independent of link length.

A key differentiator in these outcomes is the physical-layer modeling and resource configuration strategy of each method. In DO-based algorithms, all links are pre-configured for C+L-band operation, which results in lower GSNR due to broader amplifier bandwidths and increased ASE noise. In contrast, PaYG-based approaches begin with only the C-band enabled, gradually upgrading to C+L-band as needed. This selective upgrade results in higher initial GSNR levels, particularly on links operating exclusively in the C-band. Consequently, more spectrally

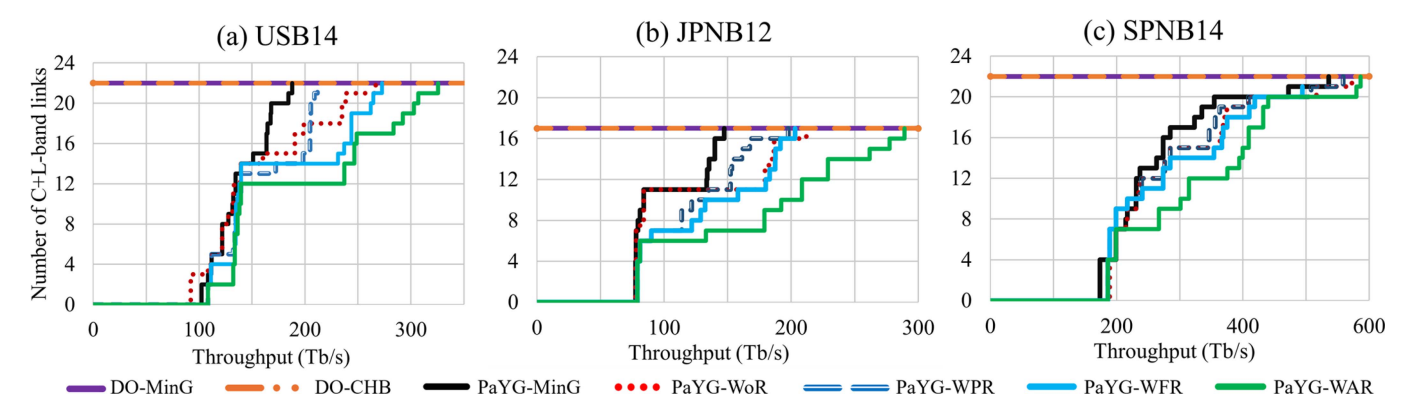


Fig. 7. Number of links upgraded to C+L-band during network growth.

TABLE V
BLOCKING RATES (%) FOR SELECTED ALGORITHMS ACROSS CONSIDERED TOPOLOGIES AT 350 TB/S THROUGHPUT

Algorithm	USB14	JPNB12	SPNB14
DO-MinG	10.55	13.92	0.07
DO-CHB	5.75	12.37	0.02
PaYG-WPR	10.78	13.96	0.11
PaYG-WFR	5.41	11.89	0.04
PaYG-WAR	2.30	6.42	0.0004

efficient modulation formats can be employed, leading to greater per-channel capacity and allowing the network to accommodate a larger number of demands before reaching blocking thresholds. Table V supports these findings by summarizing blocking rates across topologies. It emphasizes how GSNR sensitivity, channel capacity modeling, and path diversity impact each algorithm differently depending on the network structure.

2) Techno-Economic Study: In this subsection, we compare all proposed DO and PaYG algorithms in terms of CAPEX. The CAPEX is ultimately reported as the cost unit (CU) per 100 Gb/s versus the established traffic (Throughput). Calculations are based on the cost model proposed in [4]. CAPEX includes the cost of LCIs, ROADM-on-Blade cards, MCSs, and ILAs with respective CUs of 2.5, 1.9, 0.8, and 0.7. The premium factor for L-band components is set at 20%.

Fig. 7 illustrates the progression of the number of C+L-band links during network upgrading. The quantity of C+L-band links has a direct influence on the count of RoBs and ILAs, and it correlates with the number of MCSs in the network. Our strategy aims to prevent upgrading links to C+L-band whenever possible within our network. To achieve this, we maintain the network infrastructure in the C-band until there are no feasible options in existing paths to accommodate new demands. Subsequently, we upgrade the candidate links based on the algorithms outlined in Section IV to support additional demands. In Fig. 7, it is evident that the DO algorithm initially incorporates C-band and L-band infrastructure. Among the PaYG algorithms, PaYG-WoR is the first algorithm to upgrade its links from C-band to C+L-bands, while PaYG-WPR, PaYG-WFR, and PaYG-WAR are the last algorithms to undergo this upgrading. However,

in subsequent stages, the PaYG-WAR emerges as the most effective in upgrading the network. It's noteworthy that in some instances, PaYG-WFR and PaYG-WAR exhibit similarities, with PaYG-WFR demonstrating slightly superior performance. On average, according to the Monte Carlo simulation, assuming the establishment of each demand as one step, in over 95 percent of steps, the number of C+L links in PaYG-WAR is lower than in PaYG-WFR. To obtain the desired results, we allowed the networks to expand to their maximum component capacity. To determine the number of C+L links under a specific blocking rate, it is first necessary to ascertain the throughput at that particular blocking rate, as shown in Fig. 6. Once the throughput is established, we can calculate the corresponding number of C+L-band links, as depicted in Fig. 7.

As previously mentioned, the number of links directly correlates with the number of infrastructure components in both C and L bands. Fig. 8 provides insights into the growth of RoBs, MCSs, and ILAs over time. In this figure, each column corresponds to one of the networks, while each row represents a different type of infrastructure component. Observing this figure reveals that the PaYG-WAR algorithm, which upgrades the network as the last one, exhibits a lower count of RoBs and ILAs compared to other algorithms. A similar behavior is observed in PaYG-WFR. However, in certain scenarios, the number of L-band MCSs in PaYG-WFR is less than in PaYG-WAR because the latter attempts to shift as many channels as possible to the L-band, consequently increasing the number of L-band MCS. Analyzing other algorithms, except for the DO algorithms, which consistently require more infrastructure, PaYG-MinG necessitates an earlier upgrade than other algorithms. Additionally, in PaYG-WPR, although only extra bitrate is moved to the L-band, resulting in fewer MCSs in the L-band, the number of C-band MCSs is higher than WFR and WAR. The blocking rate is also higher than other algorithms because the feasible region for reconfiguration of partially C+L-band channels is narrower than WFR and WAR.

As previously discussed, the final parameter under consideration in our analysis pertains to the number of LCIs in both the C-band and L-band. Notably, the L-band LCIs are acknowledged as being more costly compared to their C-band counterparts, prompting a strategic preference for increased utilization of C-band LCIs over L-band LCIs. As shown in Fig. 8(g), (h), (i), the number of ILAs required during network upgrading is

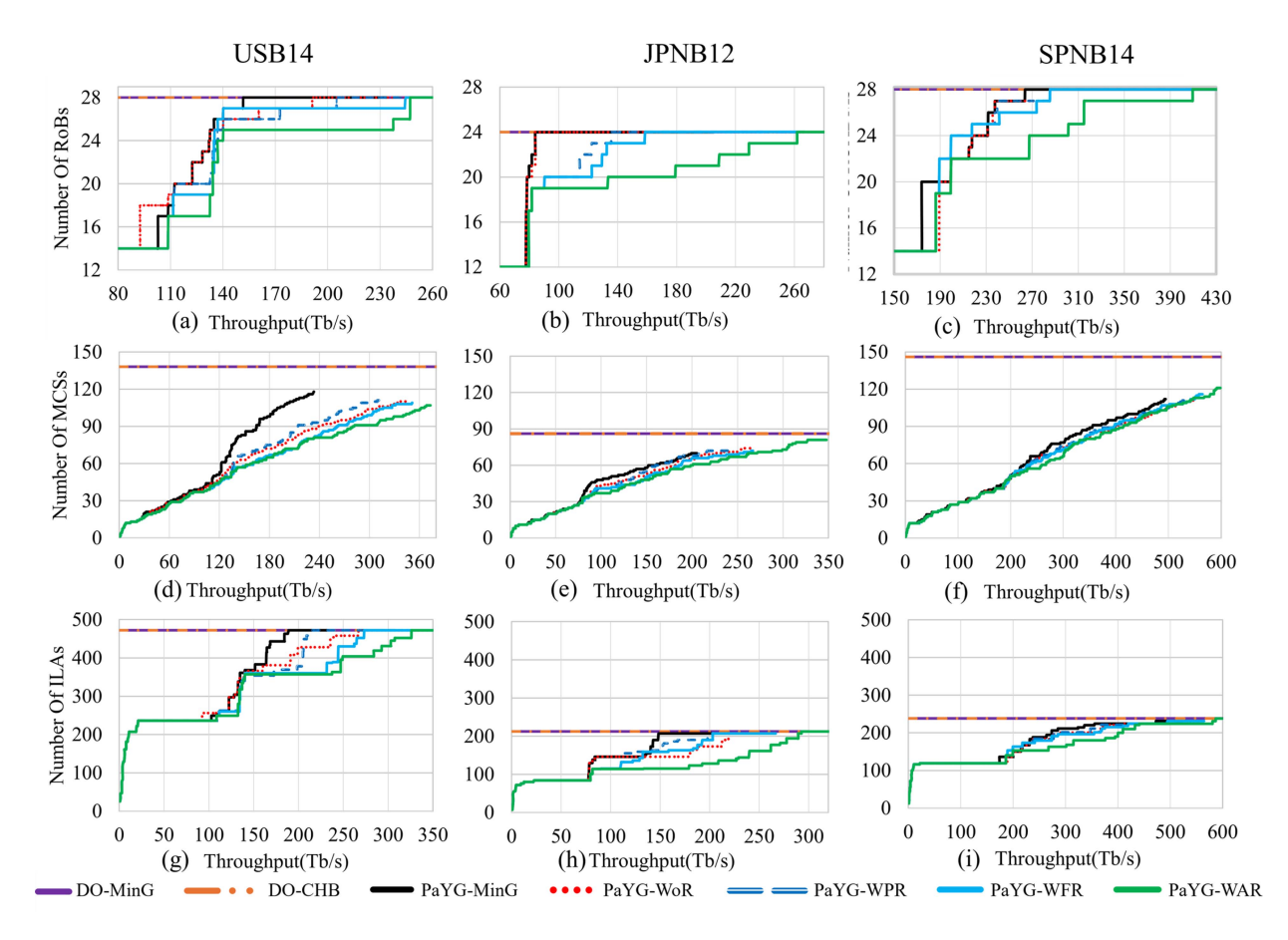


Fig. 8. Number of C-band and L-band components (RoBs, MCSs, and ILAs) deployed at varying traffic rates.

presented. Because longer links require more ILAs, these figures also provide a scale for assessing the relative lengths of upgraded links across different topologies. Fig. 9 visually illustrates the distribution of C-band and L-band LCIs. Before delving into the comparison of these figures, it's crucial to acknowledge that evaluating all algorithms at a specific throughput introduces complexities in fairness. To illustrate, consider a scenario where algorithms are scrutinized at a throughput of 270 Tb/s. At this juncture, all algorithms, except PaYG-WAR, exhibit blocking rates exceeding one percent of demands. In certain instances, this figure surpasses five percent. These algorithms tend to favor demands aligning closely with their spatial characteristics, potentially leading to the selection of shorter paths. In contrast, PaYG-WAR distinguishes itself by accommodating all demands without any instances of blocking, even at this heightened throughput. Despite variations in blocking percentages, it is noteworthy that the total established bitrate remains constant across all algorithms. This thorough examination, taking into account factors like cost, blocking tendencies, and overall throughput, emphasizes the importance of a comprehensive evaluation that goes beyond singular metrics. As we delve into these findings, a more intricate understanding of the nuances in algorithmic performance becomes apparent, revealing insights into their effectiveness and limitations across diverse operational scenarios.

As shown in Figs. 8 and 9, each link upgrade leads to a sharp rise in RoBs, MCs, ILAs, and LCIs. RoBs depend on node and link connectivity, while ILAs increase based on the number of spans, which is determined by the length of the upgraded link. LCIs grow with the number of reconfigurations, which are more frequent when longer links cause greater GSNR degradation—ultimately leading to larger increases in both LCIs and MCs.

Based on the results, the optimal choices before comparing LCIs are PaYG-WAR, PaYG-WFR, and PaYG-WoR, warranting focused attention. PaYG-WFR and PaYG-WoR show similar outcomes, while PaYG-WAR, initially aligned with them, requires more LCIs under heavy traffic due to its lower demand blocking rate, necessitating intricate spacing. Each algorithm has distinct advantages and drawbacks, requiring careful trade-off evaluation. The number of reconfigurations is also critical. While less costly than components like RoBs, MCSs, ILAs, and LCIs, reconfigurations can challenge networks, especially in terms of time. Thus, analyzing reconfigurations is essential.

Before delving into the number of reconfigurations, summarizing our comparison in throughput and the number of components is essential. The DO algorithms are known as the most costly in terms of all components, with throughput only surpassing PaYG-MinG. For other PaYG algorithms, some exhibit similar performance to DO algorithms, while others surpass them. Except for PaYG-MinG, all other PaYG algorithms

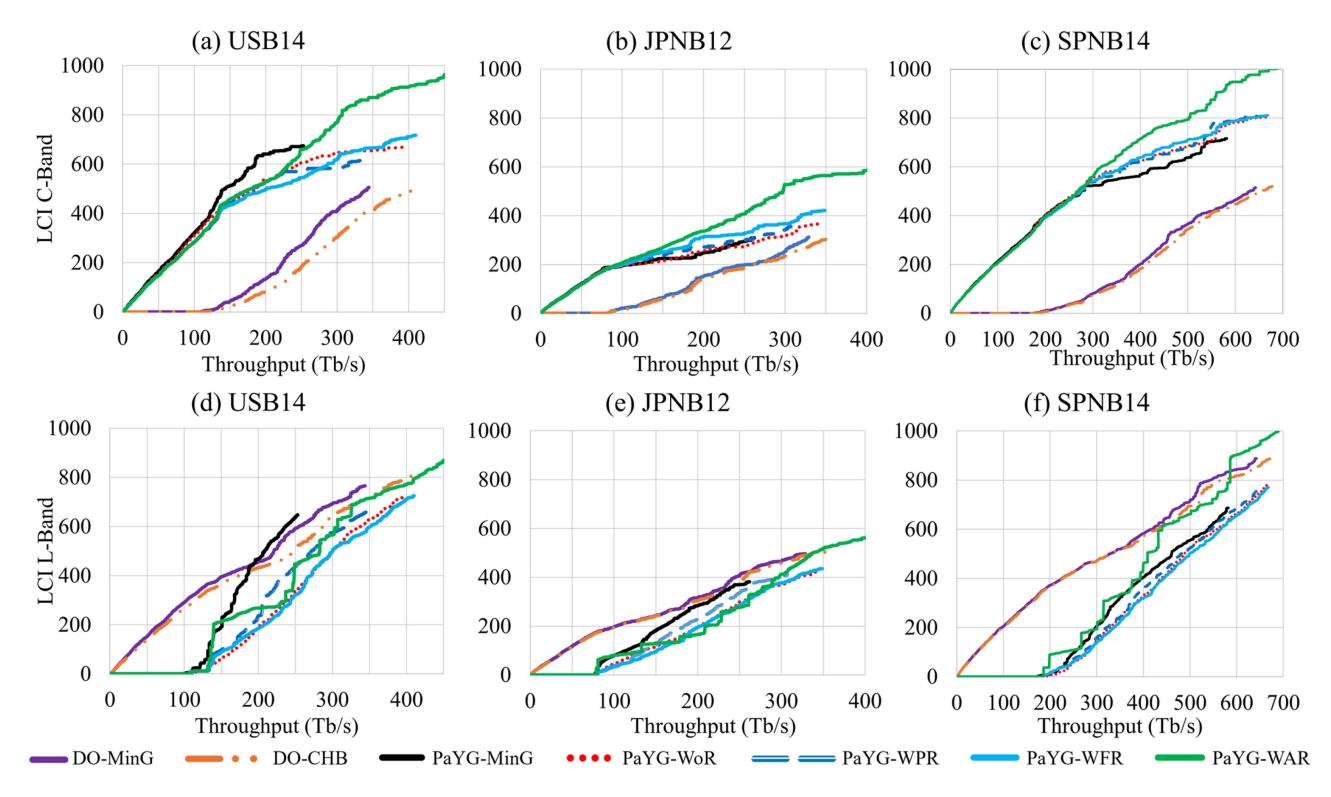


Fig. 9. Number of C-band and L-band LCIs deployed at varying traffic rates.

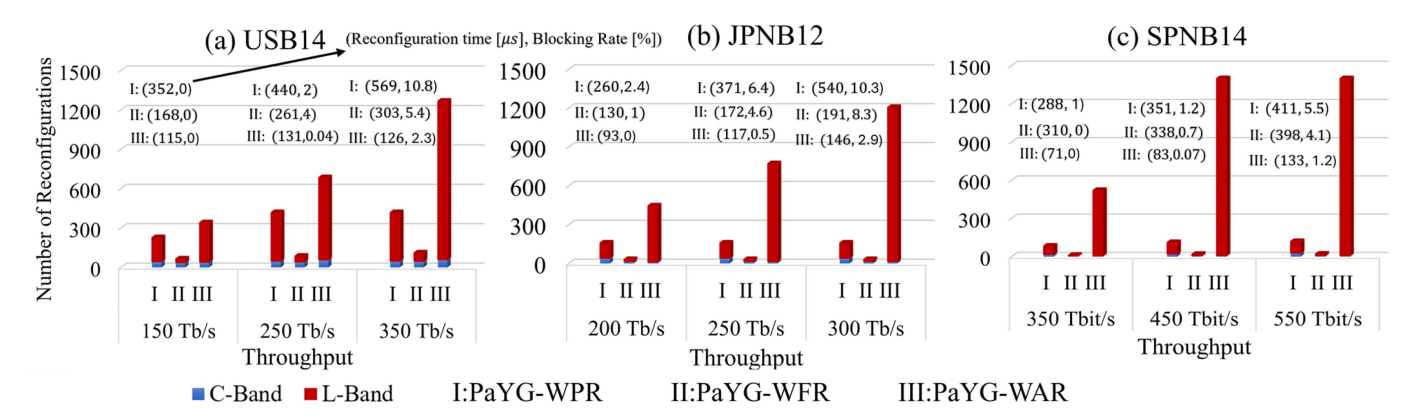


Fig. 10. Number of reconfigured channels to either C-band or L-band channels for three different established traffic values.

outperform DO algorithms in terms of CAPEX aspects. Among the PaYG algorithms, the best choices in terms of throughput and infrastructure are PaYG-WAR and PaYG-WFR, followed by PaYG-WoR. Additionally, PaYG-WoR distinguishes itself by not requiring channel reconfiguration during network upgrading, making it an attractive choice compared to PaYG-WFR and PaYG-WAR.

Fig. 10 presents a comparison of the number of reconfigurations among different algorithms. As networks designed using the DO algorithms, PaYG-MinG and PaYG-WoR, exhibit no reconfigurations, the focus in this figure is on comparing PaYG-WPR, PaYG-WFR, and PaYG-WAR. To ensure a fair assessment, we examine three snapshots of the networks. The established bitrate varies across different networks, offering a

unique snapshot of each network's characteristics. We observe the network in three distinct states to capture its behavior at various growth stages: (i) Upgrading Phase: during this stage, numerous demands have been established, and the network still possesses sufficient channel capacity to accommodate new demands. (ii) Critical Situation: the network is in a critical state, experiencing high traffic volume. In this state, we assume the blocking rate remains around one percent for most algorithms. (iii) High Throughput: representing the system at full capacity, this state reflects the network's performance under higher throughput conditions.

These specific scenarios were strategically selected to provide a comprehensive understanding of network dynamics across various growth phases, ranging from expansion and high-traffic

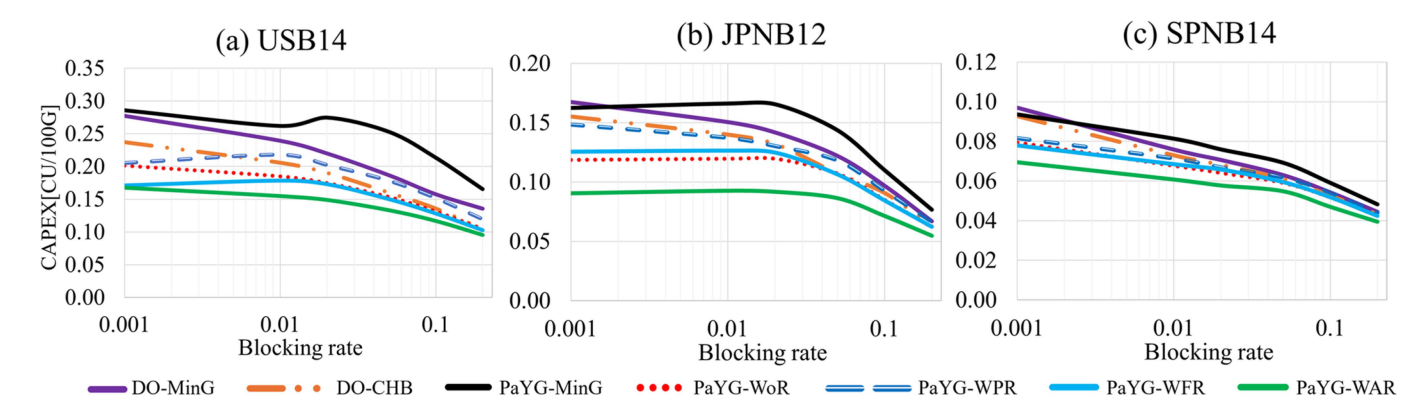


Fig. 11. CAPEX [CU/100G] for different approaches.

periods to reaching maximum capacity. The figure also illustrates the blocking rate and reconfiguration time required during network growth to achieve the specified throughput levels. As the network expands, link upgrades are attempted, though not all attempts are successful. Therefore, the total upgrading time includes both successful and failed upgrade and reconfiguration attempts. Networks utilizing more efficient algorithms with higher upgrade success rates can achieve shorter upgrade times, thereby reducing the processing time per reconfiguration.

Analyzing Fig. 10, we observe that although PaYG-WAR involves the highest number of reconfigurations, these adjustments effectively manage the blocking rate while maintaining acceptable throughput. Despite the increased reconfiguration frequency, the time per reconfiguration is reduced. As demonstrated in Fig. 10, PaYG-WAR requires fewer upgraded links and experiences fewer failed upgrade attempts than other approaches, leading to more efficient processing. Among these algorithms, PaYG-WFR performed the fewest reconfigurations during network growth. While reconfigurations increase computational overhead, they do not impact CAPEX.

To summarize the cost of each algorithm, in Fig. 11, CAPEX [CU/100G] is calculated after each demand establishment for different blocking rates. As discussed, we assumed that L-band infrastructures are 20 percent more expensive than C-band to simulate a near-real scenario. As shown, the DO-CHB (-MinG) approaches exhibit over 33% (54%) higher CAPEX compared to PaYG-WAR at a 1% blocking rate in the USB14 network. Moreover, at the same blocking rate, the CAPEX for PaYG-MinG, PaYG-WPR, PaYG-WoR, and PaYG-WFR surpass that of PaYG-WAR by 70%, 40%, 20%, and 15%, respectively, in the USB14 network. This benefit is also observed in other networks. While CAPEX improvement may vary based on topology, PaYG-WAR consistently offers a better cost per established demand in all networks. After PaYG-WAR, the PaYG-WoR and PaYG-WFR approaches demonstrate the best cost efficiency.

Table VI summarizes the performance of different algorithms across key evaluation metrics using a rating system where a higher number of + symbols indicates better performance. The results highlight the strengths and weaknesses of each approach, providing a clear comparison of their effectiveness in terms of throughput, resource efficiency, and cost. PaYG-WAR

TABLE VI KEY ADVANTAGES OF THE MODELS

	DO-MinG	ро-снв	PaYG-MinG	PaYG-WoR	PaYG-WPR	PaYG-WFR	PaYG-WAR
Blocking Rate VS	-	++	-	++	+	++	+++
Traffic Load							
(C+L Links Count)			-	+	+	++	+++
Vs Throughput							
Number of RoB,	-	-	+	++	+	++	+++
MCS and ILA							
Number of LCI	-	+	-	++	+	++	+
CAPEX	-	-	-	++	+	++	+++

consistently outperforms other methods, achieving the highest ratings across multiple criteria, while traditional DO-based methods show limited efficiency. This underscores the advantages of reconfiguration-based approaches in optimizing network performance. Although PaYG-WAR involves frequent reconfigurations, it compensates with low-complexity calculations and rapid execution, allowing it to handle reconfigurations concurrently and efficiently.

VI. CONCLUSION

In conclusion, this research delivers a sophisticated, costconscious roadmap, for the seamless transition of Elastic Optical Networks to C+L-band architectures. By meticulously integrating legacy-aware band integration (LABI) techniques with a refined PaYG framework, the study surpasses conventional upgrade strategies. The rigorous analysis, employing the enhanced generalized Gaussian noise (EGGN) model to precisely capture non-linear impairments, particularly ISRS, under diverse network topologies, reveals the remarkable efficacy of the proposed PaYG-WAR algorithm. This algorithm demonstrably optimizes throughput while simultaneously minimizing Capital expenditure (CAPEX) through strategic deployment of C+L-band components. Unlike DO approaches, PaYG-WAR dynamically adapts to evolving traffic demands, ensuring continuous service availability and optimizing resource utilization. The findings underscore the critical need for a nuanced approach to C+L-band network evolution that integrates sophisticated modeling with adaptive, cost-effective upgrade strategies. The proposed methodology offers telecommunications providers a robust and scalable solution for future-proofing their networks while mitigating the financial and operational challenges inherent in large-scale infrastructure transformations.

REFERENCES

- [1] A. Napoli et al., "Towards multiband optical systems," in Advanced Photonics 2018 (BGPP, IPR, NOMA NP, Sensors, Networks, SPPCom, SOF). Washington, DC, USA: Optica Publishing Group, 2018, p. NeTu3E.1. [Online]. Available: https://opg.optica.org/abstract.cfm?URI=Networks-2018-NeTu3E.1
- [2] A. Al-Fuqaha, M. Ayyash, M. Guizani, M. Mohammadi, and M. Aledhari, "Toward a new internet for the smart world: The convergence of IoT, edge, and 6G," *IEEE Commun. Mag.*, vol. 58, no. 7, pp. 12–17, Jun. 2021.
- [3] T. Hoshida et al., "Ultrawideband systems and networks: Beyond C L-band," *Proc. IEEE*, vol. 110, no. 11, pp. 1725–1741, Nov. 2022.
- [4] F. Arpanaei et al., "Enabling seamless migration of optical metro-urban networks to the multi-band: Unveiling a cutting-edge 6D planning tool for the 6G era," J. Opt. Commun. Netw., vol. 16, no. 4, pp. 463–480, 2024.
- [5] J. J. O. Pires, "On the capacity of optical backbone networks," *Network*, vol. 4, no. 1, pp. 114–132, 2024. [Online]. Available: https://www.mdpi.com/2673-8732/4/1/6
- [6] I. Corporation, "C 1 solution: Extending the capacity of optical networks," 2023. Accessed: Sep. 9, 2024. [Online]. Available: https://www.infinera.com/wp-content/uploads/Infinera-C-Plus-L-Solution-0345-AN-RevA-0623.pdf
- [7] A. Souza, N. Costa, J. Pedro, and J. Pires, "Comparative assessment of S C L-band and E C L-band systems with hybrid amplification," in *Proc.* 2024 Opt. Fiber Commun. Conf. Exhib., 2024, pp. 1–3.
- [8] A. Souza et al., "Cost analysis of ultrawideband transmission in optical networks," J. Opt. Commun. Netw., vol. 16, no. 2, pp. 81–93, Feb. 2024.
- [9] R. K. Jana et al., "When is operation over C + L bands more economical than multifiber for capacity upgrade of an optical backbone network?," in *Proc. Eur. Conf. Opt. Commun.*, 2020, pp. 1–4.
- [10] R. Kumar Jana et al., "Multifiber vs. ultra-wideband upgrade: A technoeconomic comparison for elastic optical backbone network," in *Proc.* 2022 Eur. Conf. Opt. Commun., 2022, pp. 1–4.
- [11] R. K. Jana, A. Srivastava, A. Lord, and A. Mitra, "Optical cable deployment versus fiber leasing: An operator's perspective on capEX savings for capacity upgrade in an elastic optical core network," *J. Opt. Commun. Netw.*, vol. 15, no. 8, pp. C179–C191, 2023.
- [12] J. P. Fernández-Palacios, F. Arpanaei, J. M. Rivas-Moscoso, J. A. Hernández, and D. Larrabeiti, "Investigation of mid-term migration scenarios to multi-band solutions in metropolitan networks," in *Proc. 23rd Int. Conf. Transparent Opt. Netw.*, 2023, pp. 1–4.
- [13] T. Ahmed, A. Mitra, S. Rahman, M. Tornatore, A. Lord, and B. Mukherjee, "C+L-band upgrade strategies to sustain traffic growth in optical backbone networks," *J. Opt. Commun. Netw.*, vol. 13, no. 7, pp. 193–203, 2021.
- [14] T. Ahmed et al., "C to C + L bands upgrade with resource re-provisioning in optical backbone networks," in *Proc. 2021 Opt. Fiber Commun. Conf. Exhib.*, 2021, pp. 1–3.
- [15] R. Kalkunte et al., "GSNR-aware resource re-provisioning for C to C + L-bands upgrade in optical backbone networks," *Photon. Netw. Commun.*, vol. 47, no. 3, pp. 139–153, 2024. [Online]. Available: https://link.springer. com/article/10.1007/s11107-024-01023-6
- [16] F. Arpanaei, J. M. Rivas-Moscoso, J. A. Hernández, J. P. Fernández-Palacios, and D. Larrabeiti, "Migration strategies from C-band to C + L-band/multi-fiber solutions in optical metropolitan area networks," in *Proc. 49th Eur. Conf. Opt. Commun.*, 2023, pp. 1–4.

- [17] Ciena.com, "A model for business case analysis of c/l-band network architectures in fiber optic networks based on leased/iru dark fiber," 2021. [Online]. Available: https://www.ciena.com/insights/white-papers/a-model-for-business-case-analysis-of-c-l-band-betwork-architectures.html
- [18] A. Souza et al., "Optimal pay-as-you-grow deployment on s CL multi-band systems," in *Proc. Opt. Fiber Commun. Conf.*, 2022, pp. W3F–4.
- [19] S. Petale et al., "PRODIGY+: A robust progressive upgrade approach for elastic optical networks," *J. Opt. Commun. Netw.*, vol. 16, no. 9, pp. E48–E60, 2024.
- [20] S. K. Patri, A. Autenrieth, J.-P. Elbers, and C. Mas-Machuca, "Multi-band transparent optical network planning strategies for 6g-ready European networks," *Opt. Fiber Technol.*, vol. 74, 2022, Art. no. 103118. [Online]. Available: https://www.sciencedirect.com/science/article/pii/S1068520022003017
- [21] S. K. Patri, A. Paz, M. Wenning, J. Muller, and C. Mas-Machuca, "Long-term upgrade strategies in multiband and multifiber optical transport networks," *J. Opt. Commun. Netw.*, vol. 16, no. 5, pp. 602–612, 2024.
- [22] M. Nakagawa, T. Seki, and T. Miyamura, "Techno-economic potential of wavelength-selective band-switchable OXC in S+C+L band optical networks," in *Proc. 2022 Opt. Fiber Commun. Conf. Exhib.*, 2022, pp. 01–03.
- [23] F. Arpanaei et al., "Synergizing hyper-accelerated power optimization and wavelength-dependent QoT-aware cross-layer design in next-generation multi-band EONs," *IEEE J. Sel. Areas Commun.*, vol. 43, no. 5, pp. 1840–1855, May 2025.
- [24] F. Arpanaei et al., "Hyperaccelerated power optimization in multi-band elastic optical networks," presented at the Opt. Fiber Commun. Conf. Exhib., San Diego, CA, USA, Mar. 24–28, 2024, Paper Th11.6.
- [25] Infinera, "Infinera ice-X portfolio of intelligent coherent pluggables," Infinera Website, 2024. [Online]. Available: https://www.blueally.com/wpcontent/uploads/2024/04/BlueAlly-branded-Infinera-ICE-X-Solution-Brief_a-FINAL.pdf
- [26] J. Cho and P. J. Winzer, "Probabilistic constellation shaping for optical fiber communications," *J. Lightw. Technol.*, vol. 37, no. 6, pp. 1590–1607, Mar. 2019.
- [27] F. Arpanaei et al., "Launch power optimization for dynamic elastic optical networks over C+L bands," in *Proc. 27th Int. Conf. Opt. Netw. Des. Modelling (ONDM 2023)*, Coimbra, Portugal, 2023, pp. 1–4.
- [28] V. Curri, "Multiband optical transport: A cost-effective and seamless increase of network capacity," in OSA Advanced Photonics Congress 2021, pp. NeTu2C-3.
- [29] Infinera, "The seven vectors of roadm evolution. Inifinera Whitepapers," (n.d.). Accessed: Nov. 2021. [Online]. Available: https://www.infinera.com/wp-content/uploads/The-Seven-Vectors-of-ROADM-Evolution-0302-WP-RevA-1121.pdf
- [30] P. Poggiolini and M. Ranjbar-Zefreh, "Closed form expressions of the nonlinear interference for UWB systems," in *Proc.* 2022 Eur. Conf. Opt. Commun., 2022, pp. 1–4.
- [31] Y. Jiang et al., "Performance enhancement of long-haul C+L+S systems by means of CFM-assisted optimization," in *Proc. 2024 Opt. Fiber Commun. Conf. Exhib.*, pp. M1F–2.
- [32] Y. Jiang et al., "Experimental test of a closed-form EGN model over C L bands," J. Lightw. Technol., vol. 43, no. 2, pp. 439–449, Jan. 2025.
- [33] P. Poggiolini, G. Bosco, A. Carena, V. Curri, Y. Jiang, and F. Forghieri, "The GN-model of fiber non-linear propagation and its applications," *J. Lightw. Technol.*, vol. 32, no. 4, pp. 694–721, Feb. 2014.
- [34] J. Pedro, N. Costa, and S. Sanders, "Cost-effective strategies to scale the capacity of regional optical transport networks," *J. Opt. Commun. Netw.*, vol. 14, no. 2, pp. A154–A165, Feb. 2022.
- [35] D. G. Sequeira, L. G. Cancela, and J. L. Rebola, "Impact of physical layer impairments on multi-degree CDC ROADM-based optical networks," in *Proc. Int. Conf. Opt. Netw. Des. Model.*, 2018, pp. 94–99.
- [36] R. Sadeghi et al., "Transparent vs translucent multi-band optical networking: Capacity and energy analyses," *J. Lightw. Technol.*, vol. 40, no. 11, pp. 3486–3498, Jun. 2022.